Published in final edited form as:
Magn Reson Med. 2008 December ; 60(6): 1512–1517. doi:10.1002/mrm.21770.

Single-shot Multi-echo Parallel EPI for DTI with Improved SNR and Reduced Distortion

Roger Nana[1], **Tiejun Zhao**[2], and **Xiaoping Hu**[1]

[1] The Wallace H. Coulter Department of Biomedical Engineering, Georgia Institute of Technology/ Emory University, Atlanta, GA 30322

[2] Siemens Medical Solutions USA, Malvern, PA 19355

Abstract

In this work, a multi-echo parallel echo planar imaging (EPI) acquisition strategy is introduced as a way to improve the acquisition efficiency in parallel diffusion tensor imaging (DTI). With the use of an appropriate echo combination strategy, the sequence can provide a signal-to-noise ratio (SNR) enhancement while maintaining the advantages of parallel EPI. Simulations and *in vivo* experiments demonstrate that a weighted summation of multi-echo images provides a significant gain in SNR over the first echo image. It is experimentally demonstrated that this SNR gain can be utilized to reduce the number of measurements often required to ensure adequate SNR for accurate DTI measures. Furthermore, the multiple echoes can be used to derive a T2 map, providing additional information that might be useful in some applications.

Keywords

Diffusion tensor imaging; diffusion weighted imaging; parallel imaging; GRAPPA; artifact reduction; SNR improvement

INTRODUCTION

Diffusion tensor imaging (DTI) (1) permits noninvasive characterization of water self-motion in tissue and thereby provides information regarding the architecture and microstructure of a tissue. DTI has been proven to be an invaluable tool for the diagnosis of pathologies that modify tissue integrity (2). Characterization of water diffusion requires a set of diffusion-weighted (DW) images (3), acquired with diffusion gradients applied in at least six non-collinear directions, plus an image with negligible diffusion weighting (*b*0 image). The greatest technical difficulty in acquiring DW images is to overcome the effects of macroscopic tissue motion, while retaining sensitivity to microscopic water motion. Owing to its insensitivity to motion, single-shot EPI (4) is the most widely used sequence for diffusion-weighted imaging (DWI). However, limited spatial resolution, sensitivity to field inhomogeneity, and low signal-to-noise ratio (SNR) are well-recognized limitations of EPI (5).

Multi-shot EPI has been used to circumvent the shortcomings of single-shot EPI (6). Multi-shot EPI reduces the off-resonance induced distortions proportionally to the number of interleaves and leads to an SNR improvement as compared to single-shot EPI. However, ghosting artifacts due to variations between shots limit its use in DWI. Due to the

Corresponding Author: Xiaoping Hu, Ph.D., The Wallace H. Coulter Dept. of Biomedical Engineering, 101 Woodruff Circle, Suite 2001, Atlanta, GA 30322, Phone: 404-712-2615, Fax: 404-712-2707, E-mail: xhu@bme.emory.edu.

complexity of brain motion and DTI's high sensitivity to motion, navigator correction (7) does not always lead to ghosting free images. In addition, DWI using multi-shot EPI has a relatively low temporal resolution and throughput, limiting its use for clinical applications.

Parallel imaging (8,9) has been demonstrated to mitigate the shortcomings of single-shot EPI effectively in general (10), as well as for DTI (11). Parallel imaging exploits the sensitivity variations of coils in a coil array to reduce the number of encoding steps necessary for gradient-based spatial encoding. Combining parallel imaging with EPI provides the advantages of a multi-shot EPI without the need of multi-shot but potentially compromises the SNR due to shortened readout and g-factor (8). Any compromise in SNR is detrimental for DTI since SNR is often limited in DTI. Therefore, it is highly desirable to improve the SNR in parallel diffusion-weighted EPI.

Multiple spin-echo or gradient-echo non-EPI acquisition strategies have been previously applied to improve the SNR (12,13) in DTI; these are, however, limited to ex-vivo studies due to the sensitivity to motion of non-EPI acquisition schemes. Parallel imaging reduces the EPI acquisition window, permitting the acquisition of multiple images with multiple echoes after a single excitation. In addition to the expected gains of reduced distortion artifacts and increased spatial resolution, the multi-echo approach is expected to improve SNR, increasing data acquisition efficiency, and provide a T2 map. The present work investigates the benefits of acquiring multi-echo images using single-shot parallel EPI for DTI. For the combination of multi-echo images, weighted averaging in which the weights for each image are determined pixel-wise as the relative attenuation of its intensity to that of the first echo image is used. The improvement in SNR of this approach is characterized both by simulation and experimentally. Its practical utility is demonstrated by fractional anisotropy (FA) maps. Furthermore, high-quality T2 maps are also derived.

METHODS

Data Acquisition and Processing

Starting from a standard diffusion-weighted EPI sequence (14), a multi-echo pulse sequence was constructed by the addition of refocusing RF pulses and EPI acquisition of the resultant spin-echoes. Phase encoding gradients are rewound after each echo so that the k-space trajectories are identical for all echoes.

All *in vivo* data were collected with participants' written consent in accordance with our institutional review board policy. The experiments were performed on a 3T Siemens Tim™ whole-body MR scanner (Siemens Medical Solutions, Malvern, PA) using a 12-channel head coil for reception and the body coil for transmission. Data were acquired on six healthy subjects (average age of 28 ± 4) with an imaging resolution of 2×2 mm^2, a matrix size of 128×128, and a slice thickness of 2 mm. Imaging protocols with an acceleration factor (R) of 2, 3, and 4, respectively, were used. The following imaging parameters were used: 5 echoes with minimum possible echo spacing, TR = 3 s, bandwidth = 1954 Hz/pixel, FOV = 256 mm, 10 axial slices, $b = 1000$ s/mm^2, and 12 diffusion weighting directions (plus $b = 0$). The echo parameters used for each imaging protocol are given in Table 1. GRAPPA (9) was used for image reconstruction. Additionally, standard spin echo (SE) images with five echoes were acquired on the same slices and at the same resolution for generating T2 maps for comparison. The SE echo times corresponded to 30, 60, 90, 120, and 150 ms.

Echo combination was performed offline. FA maps were generated after distortion correction with FSL (FMRIB, Oxford, UK) which computes the apparent diffusion coefficient for each diffusion direction using only images acquired at $b = 0$ and at the desired b value. T2 maps were calculated by mono-exponential fitting of $b0$ images or the

multi-echo SE images. All custom computer programs were implemented in Matlab (The MathWorks, Inc., Natick, MA, USA).

Echo Combination Strategies and relative SNR Analysis

When multiple echo images are acquired where signals from successive images are coherent and the noises are incoherent, several strategies can be used to obtain a composite image. For the single-shot multi-echo parallel DTI acquisition, the signal strengths of later echoes are significantly attenuated as compared to the one of the first echo due to T2 decay. In this case, weighted averaged combination of echoes would achieve higher gain in SNR than simple average and is therefore considered in this study. For simulating the SNR gain, a theoretical model of the ratio of the SNR of the combined echo to the first echo is derived as follows.

The measured signal in any pixel, $\tilde{x}$, can be represented as

$$\tilde{x}_i = x w_i + \xi_i, \quad [1]$$

where x is its true signal, i represents the echo number, ξ is the noise in echo image i assumed to have mean zero, w_i is the attenuation factor of the signal intensity of echo i with respect to that of the first echo ($i = 1$), implying that $w_1 = 1$. If N echoes are acquired, the weighted average of the measured signal, with weights given by the attenuation factors, is given by

$$\tilde{y} = \frac{x}{N}\sum_{i=1}^{N}(w_i)^2 + \frac{1}{N}\sum_{i=1}^{N}\xi_i w_i, \quad [2]$$

Let the SNR be the ratio of the mean value to the standard deviation of the noise, the ratio of the SNR of the combined echo to that of the first echo is given by

$$\frac{SNR_{\tilde{y}}}{SNR_{echo1}} = \sqrt{\sum_{i=1}^{N}(w_i)^2}. \quad [3]$$

In implementing the weighted averaging, a pixel-wise mono-exponential decay of the signal intensity between echoes was assumed and T2 map was first calculated. The pixel weight was then derived according to

$$w_i(x,y) = e^{-\frac{\Delta TE_i}{T_2(x,y)}}. \quad [4]$$

where ΔTE_i is the echo spacing between echo i and echo 1, x and y are pixel coordinates. The weights were determined on $b0$ images and used for all DW images.

SNR was measured in 18 different ROIs (per subject) categorized as major white matter (WM) tracts, deep gray matter (GM) regions, cortical WM (refers to peripheral WM within the gyri), and cortical GM. These regions were identified based on FA maps and cross-

referenced with *b*0 images to avoid inclusion of CSF-filled spaces as described by others (15). Deep GM regions comprised of bilateral sections of the globus pallidus (GP), thalamus, and putamen. Deep WM ROIs included the genu and splenium of the corpus callosum, the anterior limb of the internal capsule (AIC), the posterior limb of the internal capsule (PIC), and the external capsule (EC). Five regions of cortical WM, consisting of the superior frontal gyrus (SFG), supra marginal gyrus (SMG), superior temporal gyrus (STG), middle occipital gyrus (MOG), and postcentral gyrus (PG), were considered. The cortical GM ROIs resided in gray matter of SFG, SMG, STG, MOG, and PG. The SNR was determined according to a previously described procedure (16,17) to account for the number of receivers and the noise distribution in magnitude images obtained by sum-of-squares images. The ratio of the SNR of the combined image to that of the first echo image was computed for each ROI.

RESULTS

It is evident from visual inspection that the distortions present in diffusion-weighted images acquired using a conventional DTI sequence without acceleration in the acquisition (Fig. 1a) are significantly reduced in the ones obtained using the single-shot multi-echo parallel DTI sequence with an acceleration factor of 4 (the first echo is shown)(Fig. 1b). This improvement is in good agreement with previous observations that parallel imaging reduces distortion artifacts in EPI-DTI (10,11).

The simulated (according to equation [3]) ratios of the SNR of the combined image to that of the first echo for cerebro-spinal fluid (CSF), gray matter (GM), and white matter (WM) with assumed T2 values of 2200 ms, 100 ms, and 80 ms, respectively, are shown in Fig. 2a. In generating the plots, a constant echo spacing of 24 ms (which corresponds to the experimental value used for $R = 4$, see Table 1) was assumed and the respective weights (attenuation factors) were determined using Eq. [1.4]. The CSF shows nearly no attenuation and its relative SNR contribution is approximately the square root of the number of combined echoes. The relative SNR of the combined image tapers off after 5 echoes for both GM and WM, with SNR gain plateaus at 54% and 45%, respectively.

The results of the experimental relative SNR are shown in Fig. 2b for three imaging protocols corresponding to an acceleration factor of 2, 3, and 4, respectively. Each plot reflects the average of the relative SNR across the ROIs and the subjects. These results indicate that the gain in relative SNR tapers off after about 2, 3, and 4 echoes for $R = 2$, $R = 3$, and $R = 4$, respectively. At the plateau, the relative SNR gain was $(15 \pm 2)\%$ for $R = 2$, $(25 \pm 3)\%$ for $R = 3$, and $(36 \pm 5)\%$ for $R = 4$.

Figure 3 presents FA maps of three slices (displayed in three different rows) generated (a) from a single-shot single-echo acquisition without averaging (corresponding to a scan time of 57 s), (b) a single-shot single-echo acquisition with two averages (corresponding to an acquisition time of 1 min 36 s), and (c) a single-shot 4-echo acquisition without averaging (corresponding to a scan time of 57 s). While the FA maps generated from the first echo without averaging exhibit significant noise level (Fig. 3a), the noise level in the FA maps generated from the 4 echo combination is significantly reduced (Fig. 3c), on par with that in the FA maps generated with 2 averages (Fig. 3b). Table 2 lists the mean FA values in the ROIs used for the SNR analysis. Note that for the cortical WM and cortical GM, respectively, values of individual ROIs were pooled together because they were very similar. The combination of 4 echoes led to FA values that are higher than those obtained with echo 1 without averaging and in good agreement with those obtained with echo 1 with 2 averages.

T2-weighted images (a) and the corresponding T2 maps (b) of two slices generated from 4 echoes of an $R = 4$ multi-echo dataset are shown in Fig. 4. For comparison, images of the same slices obtained using a standard multi-echo SE sequence and corresponding T2-maps are shown in panels (c) and (d), respectively. Table 3 lists the T2 values of selected ROIs compared to those obtained using the standard multi-echo SE sequence.

DISCUSSION

The numerical calculations allowed us to investigate theoretically the performance of combined image using multi-echo parallel EPI, assuming representative T2 values and practical echo spacing. The latter mainly depends on the acquired matrix size and the bandwidth per pixel. The numerical results indicate that combining multiple echoes could result in SNR improvement and that considerably larger gains are expected in regions of longer T2 or for acquisitions with short echo spacing. The experimental SNR ratio between the combined image and the first echo image (Fig. 2b) largely follow the numerical prediction (Fig. 2a). However, the height and the location of the SNR plateaus are slightly different from those of the simulations Note that at R = 4, the experimental echo-spacing ($\Delta TE = 24$ ms) corresponds to that used for simulations. These discrepancies are likely due to errors in determining the attenuation factors (w_i) and the imperfection of the refocusing RF pulses. Overall, the experimental results support the prediction that echo combination leads to a SNR gain or at least maintains the SNR for all the number of echo combinations examined in this study.

The fact that the SNR tapers off after the combination of two echoes for the acceleration factor of 2 and more echoes at higher reduction factors is understandable because the shorter echo spacing at higher R allows the inclusion of more echoes before the signal drops out due to T2 decay. The 36% SNR increase in the combined image relative to the first echo image at $R = 4$ is close to the increase of 41% that would be expected from two averages of the first echo; this gain in SNR can be used to reduce the number of measurements and thereby leading to reduced scan time. This point is supported by the FA maps shown in Fig. 3. The FA maps obtained from the first echo without averaging exhibits a significant noise level whereas the noise level of the FA maps generated from the weighted average of 4 echoes with the same acquisition time is significantly reduced, to a level comparable to that in the FA maps generated from 2 averages of the first echo. These noise level differences led to a significant difference in the FA values reported in Table 2. The first echo without averaging resulted in a decrease in anisotropy as its signal is close to the noise level (18). On the other hand, averaging the first echo with two averages or combining 4 echoes led to a better estimate of the anisotropy.

Sum of squares (SOS) is widely used to combine images from array coils and provides a near optimal combination when the SNR is high but is less than optimal at low SNR (19,20). Because multi-echo DTI images have low SNR, weighted average instead of SOS is used in this work. This choice is supported by our comparison (data not shown here) of the two methods when applied to our experimental data, which showed that weighted average performs better.

In a previous paper, Matiello *et al.* (21) reported that the contributions of EPI readout and phase-encoding gradients to the b-matrix in DTI-EPI sequence were negligible. We have performed a similar analysis, taking into account the crusher and slice selection gradients associated with refocusing RF pulses for additional echoes. With the imaging parameters used in this work, the difference in b-values between adjacent echoes ranges from 0.19 to 0.27 s/mm^2. This difference is negligible, even when multiplied by 4 for the 5th echo, compared to the nominal b-value of 1000 s/mm^2. For pixels containing multiple

compartments with different T2s, compartment-dependent T2 decay between the echoes may complicate the combination of the echoes. This was not found to be a significant factor as there is no statistically significant difference between the FA values of the echo combination and the first echo with approximately similar SNR (see Table 3).

The quality of the T2 maps derived using the single-shot multi-echo parallel EPI data (Fig. 4b) is as good as the ones obtained using the standard multi-echo SE data (Fig. 4d). Furthermore, as is illustrated in Table 3, no statistical significant differences between the corresponding T2 values probed from selected ROIs were found, consistent with the results reported in the literature (22,23). This demonstrates the potential of the single-shot multi-echo parallel diffusion weighted EPI sequence for providing additional information that might be useful in some applications.

The multi-echo approach provides more gain at high parallel imaging acceleration factors. In the past, an acceleration factor of 2 is often used for parallel imaging to avoid image degradation at high accelerations. With the availability of array coils with a large number of channels, it is now common to use higher acceleration factors, such as 3, 4, and even higher (24,25). In fact, with the 12-channel commercial array coil used in this study, images obtained using an acceleration factor of 4 are of good quality.

While the multi-echo approach can enhance SNR per excitation, it could compromise the efficiency in multi-slice acquisitions. Specifically, with a given number of slices, the minimum TR may be lengthened. In applications where a large number slices are acquired, a good approach may be to acquire 2 echoes, achieving most of the SNR gain while avoiding significantly increasing the TR.

CONCLUSION

We have implemented and demonstrated a single-shot multi-echo parallel diffusion-weighted EPI sequence in improving the SNR while retaining the advantages of reduced distortion. The SNR gain can be used to reduce the number of measurements needed or improve the image resolution. Furthermore, these additional echoes can be used to calculate the T2 map, providing complementary information that might be useful in some applications.

Acknowledgments

This work was supported in part by the National Institutes of Health (RO1EB002009) and the Georgia Research Alliance.

References

1. Basser PJ, Mattiello J, LeBihan D. MR diffusion tensor spectroscopy and imaging. Biophys J. 1994; 66(1):259–267. [PubMed: 8130344]
2. Horsfield MA, Jones DK. Applications of diffusion-weighted and diffusion tensor MRI to white matter diseases - a review. NMR Biomed. 2002; 15(7–8):570–577. [PubMed: 12489103]
3. Le Bihan D. Molecular diffusion nuclear magnetic resonance imaging. Magn Reson Q. 1991; 7(1): 1–30. [PubMed: 2043461]
4. Mansfield P, Maudsley AA, Baines T. Fast scan proton density imaging by NMR. J Phys E: Scient Instrum. 1976; 9:271.
5. Farzaneh F, Riederer SJ, Pelc NJ. Analysis of T2 limitations and off-resonance effects on spatial resolution and artifacts in echo-planar imaging. Magn Reson Med. 1990; 14(1):123–139. [PubMed: 2352469]

6. Butts K, Riederer SJ, Ehman RL, Thompson RM, Jack CR. Interleaved echo planar imaging on a standard MRI system. Magn Reson Med. 1994; 31(1):67–72. [PubMed: 8121272]
7. Anderson AW, Gore JC. Analysis and correction of motion artifacts in diffusion weighted imaging. Magn Reson Med. 1994; 32(3):379–387. [PubMed: 7984070]
8. Pruessmann KP, Weiger M, Scheidegger MB, Boesiger P. SENSE: sensitivity encoding for fast MRI. Magn Reson Med. 1999; 42(5):952–962. [PubMed: 10542355]
9. Griswold MA, Jakob PM, Heidemann RM, Nittka M, Jellus V, Wang J, Kiefer B, Haase A. Generalized autocalibrating partially parallel acquisitions (GRAPPA). Magn Reson Med. 2002; 47(6):1202–1210. [PubMed: 12111967]
10. Griswold MA, Jakob PM, Chen Q, Goldfarb JW, Manning WJ, Edelman RR, Sodickson DK. Resolution enhancement in single-shot imaging using simultaneous acquisition of spatial harmonics (SMASH). Magn Reson Med. 1999; 41(6):1236–1245. [PubMed: 10371457]
11. Jaermann T, Crelier G, Pruessmann KP, Golay X, Netsch T, van Muiswinkel AM, Mori S, van Zijl PC, Valavanis A, Kollias S, Boesiger P. SENSE-DTI at 3 T. Magn Reson Med. 2004; 51(2):230–236. [PubMed: 14755645]
12. Gulani V, Iwamoto GA, Jiang H, Shimony JS, Webb AG, Lauterbur PC. A multiple echo pulse sequence for diffusion tensor imaging and its application in excised rat spinal cords. Magn Reson Med. 1997; 38(6):868–873. [PubMed: 9402185]
13. Gulani V, Weber T, Neuberger T, Webb AG. Improved time efficiency and accuracy in diffusion tensor microimaging with multiple-echo acquisition. J Magn Reson. 2005; 177(2):329–335. [PubMed: 16185903]
14. Reese TG, Heid O, Weisskoff RM, Wedeen VJ. Reduction of eddy-current-induced distortion in diffusion MRI using a twice-refocused spin echo. Magn Reson Med. 2003; 49(1):177–182. [PubMed: 12509835]
15. Bhagat YA, Beaulieu C. Diffusion anisotropy in subcortical white matter and cortical gray matter: changes with aging and the role of CSF-suppression. J Magn Reson Imaging. 2004; 20(2):216–227. [PubMed: 15269946]
16. Kellman P, McVeigh ER. Image reconstruction in SNR units: a general method for SNR enhancement. Magn Reson Med. 2005; 54(6):1439–1447. [PubMed: 16261576]
17. Eratum to Kellman P, McVeigh ER. Image reconstruction in SNR units: a general method for SNR enhancement. Magn Reson Med. 2005; 54(6):1439–1447. [PubMed: 16261576] Magn Reson Med. 2007; 58(1):211–212.
18. Jones DK, Basser PJ. “Squashing peanuts and smashing pumpkins”: how noise distorts diffusion-weighted MR data. Magn Reson Med. 2004; 52(5):979–993. [PubMed: 15508154]
19. Larsson EG, Erdogmus R, Yan JCP, Fitzsimons. SNR-optimality of sum-of-squares reconstruction for phased array magnetic resonance imaging. J Magn Reson. 2003; 163:121–123. [PubMed: 12852915]
20. Gilbert G, Simard D, Beaudoin G. Impact of an improved combination of signals from Array coils in diffusion tensor imaging. IEEE Trans Med Imaging. 2007; 26(11):11428–1436.
21. Mattiello J, Basser PJ, Lebihan D. The b matrix in diffusion tensor echo-planar imaging. Magn Reson Med. 1997; 37(2):292–300. [PubMed: 9001155]
22. Jezzard P, Duewell S, Balaban RS. MR relaxation times in human brain: measurement at 4 T. Radiology. 1996; 199(3):773–779. [PubMed: 8638004]
23. Rohan, ML.; Eskesen, JG.; Anderson, CM.; Kaufman, MJ.; Renshaw, PF. TE Stepping with EPI: Reliable Relaxometry. Proc of the Annual Meeting of ISMRM; Kyoto. 2004. p. 993
24. Zhu Y, Hardy CJ, Sodickson DK, Giaquinto RO, Dumoulin CL, Kenwood G, Niendorf T, Lejay H, McKenzie CA, Ohliger MA, Rofsky NM. Higly parallel volumetric imaging with 32-element RF coil array. Magn Reson Med. 2004; 52(4):869–877. [PubMed: 15389961]
25. McDougall PM, Wright SM. 64-channel array coil for single echo acquisition magnetic resonance imaging. Magn Reson Med. 2005; 54(2):386–392. [PubMed: 16032696]

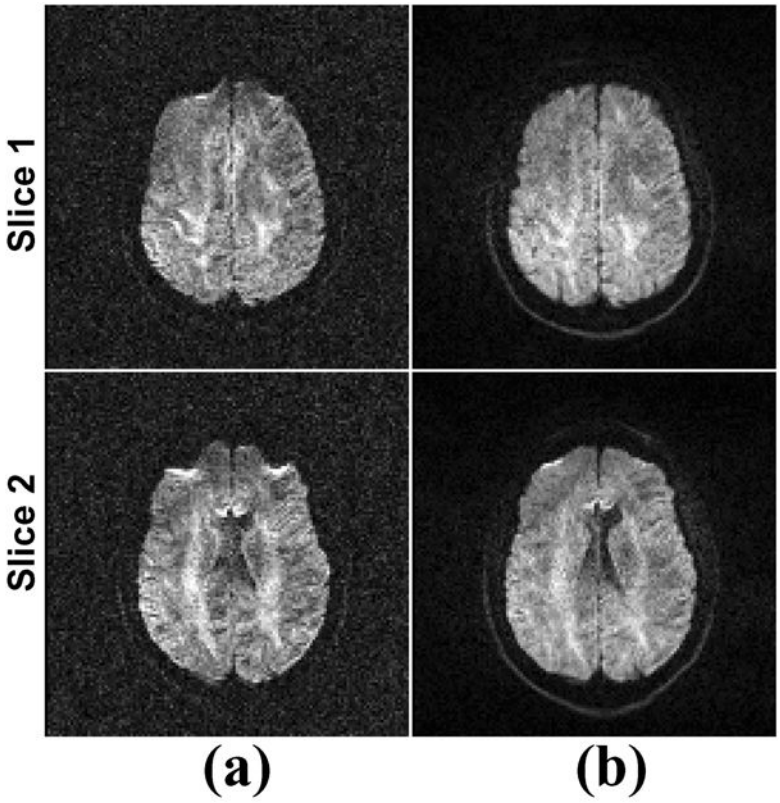

Figure 1.
Diffusion-weighted Images acquired using (a) a standard diffusion sequence without parallel imaging with TE = 132 ms and (b) single-shot multi-echo parallel DTI sequence with acceleration factor of 4 (only the first echo image acquired at TE = 80 ms is shown). In both cases, b = 1000 s/mm^2. The distortion artifacts present in the images of column (a) are significantly reduced in those of column (b).

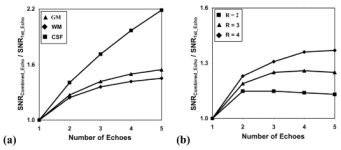

Figure 2.

(a) Numerically derived ratio of the SNR of the echo combination to that of the first echo alone plotted as a function of the number of echoes combined, assuming a constant echo spacing of 24 ms and a T2 of 2200 ms, 100 ms, and 80 ms for cerebro-spinal fluid (CSF), gray matter (GM), and white matter (WM), respectively. (b) Experimental plots of the relative SNR change between the echo combination and the first echo as a function of the number of echoes for three different parallel imaging protocols corresponding to $R = 2$, $R = 3$, and $R = 4$, respectively. Each plot reflects the average of the relative SNR across the ROIs and the subjects.

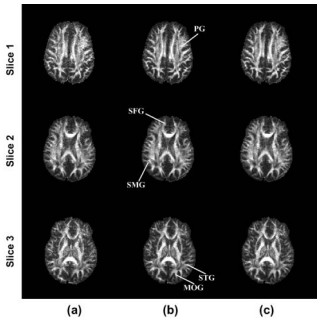

Figure 3.
Comparison between FA maps generated from multi-echo DTI datasets (R = 4) of 3 slices of a healthy subject from: (a) first echo without averaging; (b) first echo with 2 averages; (c) combination of four echoes of a single excitation without averaging.

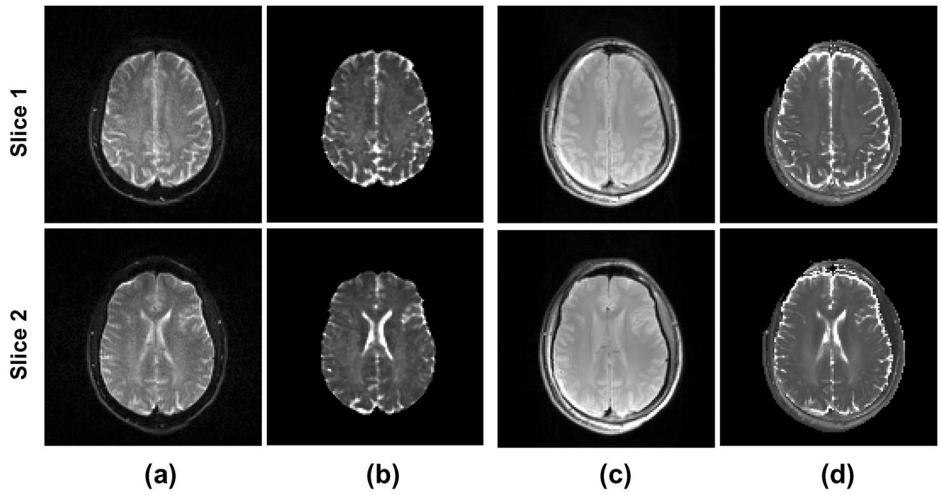

Figure 4.
b0 images (column a) and corresponding T2 maps (Column b) generated from 4 echoes of a single excitation multi-echo DTI dataset (R = 4). SE images obtained on the same slices and corresponding T2 maps are shown in columns c and d, respectively.

Table 1

Echo times used for different acceleration factors.

R	TE(1) (ms)	TE(2) (ms)	TE(3) (ms)	TE(4) (ms)	TE(5) (ms)
2	96	141	186	231	276
3	85	117	149	181	213
4	80	104	128	156	184

Table 2

Comparison between FA values of 18 selected ROIs obtained from the same datasets as in Fig. 3.

Region	FA values		
	1st echo image without averaging	1st echo image with 2 averages	Weighted average combination of 4 echoes
Combined cortical white matter	0.38 ± 0.05	0.46 ± 0.04	0.43 ± 0.03
Combined cortical gray matter	0.17 ± 0.06	0.21 ± 0.02	0.20 ± 0.05
Major white matter			
Genu of Corpus callosum	0.60 ± 0.04	0.65 ± 0.03	0.66 ± 0.04
Splenium of Corpus callosum	0.64 ± 0.07	0.70 ± 0.03	0.68 ± 0.03
Anterior limb-internal capsule	0.55 ± 0.05	0.60 ± 0.03	0.62 ± 0.05
Posterior limb-internal capsule	0.56 ± 0.06	0.62 ± 0.04	0.61 ± 0.04
External capsule	0.40 ± 0.05	0.47 ± 0.02	0.45 ± 0.03
Deep gray matter			
Thalamus	0.33 ± 0.05	0.37 ± 0.03	0.35 ± 0.03
Putamen	0.18 ± 0.03	0.21 ± 0.03	0.23 ± 0.03
Globus pallidus	0.26 ± 0.06	0.31 ± 0.02	0.33 ± 0.04

Table 3

Comparison between T2 values obtained using the multi-echo parallel EPI and standard SE sequences

Region	T2 Values, msec	
	Single-shot multi-echo parallel EPI	Standard SE
Cortical gray matter	70.42 ± 5.89	73.01 ± 4.53
White matter	54.71 ± 4.22	55.23 ± 3.64
Caudate Nucleus	61.95 ± 11.73	63.37 ± 9.15
Putamen	56.16 ± 9.12	57.65 ± 9.63
CSF	843 ± 206	871 ± 225